SHADOW PROCESSING TECHNOLOGY OF AGRICULTURAL PLANT VIDEO IMAGE BASED ON PROBABLE LEARNING PIXEL CLASSIFICATION
/
基于概率学习像素分类法的农业植物视频图像阴影处理技术研究

Cheng Yang[1)], *Ping* Wang[1)], *Yan* Bao[*1)] [1]
[1)] College of Electronic Information and Electrical Engineering, Changsha University, Changsha, 410022 / China
https://doi.org/10.35633/inmateh-60-23

Keywords: *probability learning; pixel classification; agricultural plants; video images*

ABSTRACT
In order to solve the problem of difficult pre-processing of crop video image shadows, a probable learning pixel classification method is proposed to study its processing technology. The algorithm effectively detects the shadow area by performing intelligent video collaborative detection on the shaded parts of the crop video sequence. Firstly, the cloud collaborative detection algorithm that can be widely used in agriculture was proposed. The video key frame was obtained and the background modeling algorithm with strong adaptability to crop illumination was applied to realize real-time detection of the target, so as to construct the crop pixel model. Finally, the proposed algorithm and the constructed model are applied to the processing of shadows of agricultural plant video images for experimental verification. The results show that in video frames 47, 194 and 258, the probable learning pixel classification method can be used to determine the shaded part of each frame, which can greatly improve the detection accuracy of crop shadows. The research in this paper shows that the probability learning pixel classification method can better enhance the shadow robustness and accuracy of crop video images.

摘要
为了解决作物视频图像阴影预处理困难的问题，提出了一种概率学习像素分类方法来研究其处理技术。该算法通过对作物视频序列的阴影部分进行智能视频协同检测，有效地检测出阴影区域。首先，提出了可广泛应用于农业领域的云协同检测算法。获取视频关键帧，采用对作物光照适应性强的背景建模算法实现对目标的实时检测，从而构建作物像素模型。最后，将所提出的算法和所构建的模型应用于农业植物视频图像的阴影处理并进行实验验证。结果表明，在 47 帧、194 帧和 258 帧中，采用概率学习像素分类方法可以确定每帧的阴影部分，大大提高了作物阴影的检测精度。本文的研究表明，基于概率学习的像素分类方法能够更好地加强作物视频图像阴影的稳定性和准确性。

INTRODUCTION
Recently, the use of information technology to bring data from different sources into decision-making related to agricultural production is the popular management strategy—precision agriculture (PA). An example of a PA application is the measurement and management of the number and space utilization of cultivated land *(Rashno A, Nazari B, Sadri S., 2017)*. Due to the development of computer technology and digital video technology, and the economic benefits of pursuing the image acquisition process, the range of video cameras used in real-time fields is gradually expanding *(Windrim L, Ramakrishnan R, Melkumyan A., 2018)*. The traditional method of regional segmentation has the method of regional growth and regional division *(Xu M, Zhu J., Lv P., 2017)*. This kind of method can segment images with a priori knowledge such as complex scenes or natural scenes without a priori knowledge, and can also achieve better performance. However, this type of method is an iterative method with large spatial and temporal overhead *(Tatar N., Saadatseresht M., Arefi H., 2018)*. In this paper, a shadow processing technique based on probable learning pixel classification method is proposed, which can effectively segment the shadow region of agricultural plant video images, which has important practical significance.

The presence of shadow will affect many subsequent agricultural image processing operations, and then affect the researchers in agriculture related research. The purpose and requirements for processing shadows in images vary from application to application *(Nan M, Zhu R., Li Y., 2018)*. In order to improve the shadow processing technology of agricultural plant video images, a *probable learning pixel classification*

---

[1] *Cheng Yang, As. Lec. Stud., Ping Wang, Lec. Stud.; Yan Bao, Assoc. Prof. Ph.D.*

method is proposed based on real-time intelligent video capture, and a crop pixel model is constructed based on cloud collaborative detection. The probability learning pixel classification method based on real-time intelligent video capture is realized by calling the interface provided by Haikang through the process of capturing video frames into images on the video server. The crop pixel model based on cloud collaborative detection algorithm estimates the value of model parameters under the condition of giving the initial value of missing data, and then estimates the missing value of crop data according to the parameters. According to the estimated crop missing data, the parameter value was updated, and repeated iterations were carried out until the convergence and the end of the iteration.

The pre-processing operations for image shading include two steps of shadow detection and shadow elimination. The innovation of this paper is to propose a video sequence processing method for shadow detection and removal. A probability learning pixel classification algorithm for the shadow distribution model is established for a pixel and sometimes a crop shadow. By combining the algorithm to store all observed image pixel values for real-time applications, real-time applied probabilistic reasoning unsupervised pixel classification is implemented, which solves the problem of difficult to handle shadow regions in the traditional image classification method.

This article applies the computer technology in the agricultural production, makes every effort to innovate the present agricultural production pattern. The probability learning pixel classification method is used to explore the agricultural plant shadow processing technology, and a crop pixel model is built based on cloud collaborative detection. Based on the video image capture, a real-time intelligent video capture algorithm is proposed, and the main model and algorithm are applied. The principle and implementation process are analyzed. Finally, the algorithm proposed in this paper is tested and the results are summarized and analyzed.

Related work

In agriculture-related early satellite remote sensing technology, images obtained from satellites or aircraft could effectively provide relevant agricultural information such as forests, cultivated land, soil and plant density. The next stage after the image was obtained was that the vegetation was segmented from the background. *Hadiuzzaman M.* used a standardized different index and morphological operations to segment plants, and found that the method was feasible *(Hadiuzzaman M,, Haque N,, Rahman F.. 2017)*. *Argandacarreras I.* designed a robust segmentation algorithm, and found that the algorithm could obtain good segmentation results under outdoor light changes *(Argandacarreras I., Kaynig V., Rueden C., 2017). Yang S*. classified broadleaf grasses and grasses using Gabor filters and artificial neural networks. The study found that this method had certain advantages *(Yang S, Feng Z., Wang M., 2018)*. *Arun P.V.* took the colour image of sugar beet field in seedling stage as the research object, and proposed a real-time agricultural image pixel-by-pixel classification method based on depth separable convolution. Compared with the existing pixel-by-pixel classification method, it was found that the method obtains high classification accuracy. *(Arun P.V., Buddhiraju K.M., Porwal A., 2018). Li J*. proposed a KmeansNet model for the classification and recognition of plant image sets. It was found that this method was a variant of the SPCANet model, except that the convolution kernel of the convolutional layer was obtained by the Kmeans algorithm *(Li J, Khodadadzadeh M., Plaza A., 2017)*. *Majdar R.S.* proposed a plant image set classification method based on deep learning. The research showed that the deep learning model with the smallest set of reconstruction errors could get the category label of the test set *(Majdar R.S., Ghassemian H., 2017)*. However, various vegetation segmentation studies did nothing to the shadows. So far, many scholars have analyzed the shadow features, established a model of shadow generation, and proposed a number of related algorithms for detecting shadow regions. *Hou B*. proposed image processing and support vector machine methods. Experiments showed that the method adapts to different illumination intensities and could reduce the influence of noise, plant shadows and debris on image segmentation, and obtain a complete segmentation image *(Hou B, Kou H., Jiao L., 2017). Sharma A.* used a variety of typical colour constancy algorithms to compare the effects of colour restoration in grape leaf images. The results showed that various algorithms had a certain effect on the consistency of leaf colour in the image *(Sharma A, Liu X., Yang X., 2018)*. *Yan X*. had many assumptions and low detection efficiency for general colour shadow detection. Based on the shadow analysis, the bottom-up method was used to detect the shadow using gradient and colour information. The simulation results showed that the shadow detection rate of this method was optimal in most cases, the average shadow discrimination rate was as high as 0.92, and the total average was 0.73. The detection effect was better than other methods *(Yan X, Lu Y., Liu L., 2018)*. *Groot H.G.J.* proposed a colour image shadow detection method. It was found that this method could effectively detect shadow areas of various intensities under complex background conditions. It had the advantages of accurate detection, fast processing speed and no need for manual intervention. It was suitable for practical applications *(Groot H.G.J., Oostdijk A., Van Persie M., 2017)*. In summary, most scholars verified the effectiveness of the algorithm through experiments. However, for image shading, some scholars have also proposed many shadow detection algorithms, and have achieved certain results. Therefore, based on the previous studies, this paper has important practical significance for the research of agricultural plant video image shadow processing technology based on probability learning pixel classification.

MATERIALS AND METHODS

Shadow processing technology of agricultural plant video image, based on probable learning pixel classification

Probable learning pixel classification based on real-time intelligent video capture

The multi-channel fast detection mechanism refers to the function of pedestrian detection when the system is deployed. It is divided into two steps when testing pedestrians. The first step is to quickly detect pedestrians in the system. The method of fast detection is a background modeling method. When the current video is larger than the background model, the video frame may be initially identified as having a potential abnormality *(Wang P, Hu X, Li Y. 2016).* The reason why the video frame is first detected in one step is because no part of the camera deployment area will occur for most of the time, such as military management areas or warehouses where pedestrians are prohibited from entering or leaving. If the video stream data in the response time of the timer is captured for a complete detection, it will waste more time to affect the video data to be forwarded to the client *(Girard F, Kavalec C, Cheriet F., 2019)*. So, the first step is to quickly detect the video data, capture the valuable video data, and then use the trained machine learning model for more accurate detection. The video data is is captured and the trained machine learning model is used for more accurate detection *(Xiao-Bing H.U., Rong-Fang Z., Xing Y.E., 2017)*. After the video streaming server starts running, the main thread will establish two sockets, which are the data port and the control port *(Yang J., Wang C., Cai G., 2016).* The video stream obtained by the server from the NVR (Network Video Recorder) is sent from the data port to the client, and the client requests the server. Both are sent from the control port to the server *(Yang J., Wang C., Xie C., 2017)*. The socket created by the main thread will always be in the listening state, listening to the client's connection request *(Tolstik T., Marquardt C., Matth Us C., 2014)*. When the connection request of the client is monitored, a connection is established with the client, and the client also sends a video request to the server through the control port. The server main thread checks its permissions according to the client's request, determines whether the client can view the video of the channel, and then the server establishes the corresponding channel *(Skakun S, Kussul N, Shelestov A.Y., 2016).* Each channel has a ring buffer and is independent of each other. Each channel reads the configuration information such as the IP (intellectual property) address, port number, user name, and password of the NVR in the database, and logs in to the NVR using the NET_DVR_Login_V30 interface. After the login is completed, the main thread will start two sub-threads, one is the forwarding sub-thread responsible for the video stream forwarding view, and the other is the capture sub-thread responsible for acquiring the key frames in the video stream.

Next, the main thread will use the NET_DVR_Real Play_V30 interface to obtain the video stream of a certain channel according to the channel number, stream type, stream taking mode, callback function and other parameters of the client request channel *(Xiao-Hong W., Yu-Qian Z., Miao L., 2015)*. The callback function is an execution function for obtaining a video stream, and the main line can obtain the code stream type and size of the video stream and the User ID of the code stream through the callback function. Through these attribute information of the code stream the main thread distributes the video stream of each channel to its own ring buffer, and then the sub thread responsible for forwarding uses the optimal forwarding algorithm in Chapter 3 to send the video stream in the buffer to the client. The sub-thread responsible for forwarding then uses the optimal forwarding algorithm in Chapter 3 to send the video stream in the buffer to the client. After the main thread obtains the callback function and the video stream is mounted on the ring buffer according to the channel number of the video frame, the same video frame is also placed in the playback buffer constructed by the server in the callback function. The capture sub-thread will set the timer at the beginning of the startup. The response interval of the timer is 1 second. During the response time, the sub-thread will obtain the video dump from the playback buffer through the above-mentioned Player Buf-based capture scheme. And then check the value of flag bit. In the case where the flag value is 1, the image is quickly detected. If the detected key frame image is dynamically changed based on the detection background, the risk of potential abnormality is considered, and the image is saved locally or continues to utilize the cloud-based machine learning model. Perform a second test.

Crop pixel model based on cloud collaborative detection algorithm

The Histogram of Oriented Gradient (HOG) is a feature of statistically analyzing the gradient direction of a local region of an image. It is commonly used for object detection in computer vision and image processing. Compared to other features, HOG has many advantages. First, the HOG operates on the local square of the image, maintaining a good invariance to both image geometry and optical distortion. Secondly, under the conditions of spatial and directional space sampling and normalization, pedestrians are allowed to have some subtle actions that do not affect the detection effect. In an image, the shape of the local target can be described by the statistical information of the gradient, so that each image is extracted by HOG, and the generated vector is used to represent the gradient statistical information. Using a 64*128 image to extract the HOG feature's practice flow: After completing the first three steps of the above process, a 16*16 pixel block and an 8*8 pixel cell are created in the 64*128 image window. Each block has 4 cells, and the number of directions of the gradient is bins=9. Histogram statistics are performed on the gradient direction of all pixels in each cell to obtain a 9-dimensional feature vector; thus, a 36-dimensional vector is obtained in each block. The sample image window is scanned with overlapping blocks, with 7 scanning areas in the horizontal direction and 15 scanning areas in the vertical direction, and all the block features are connected. Finally, a feature of 36*7*15=3780 dimensions is obtained. SVM (*Support Vector Machine*) is a VC (Vapnik–Chervonenkis) learning theory based on statistical learning theory and a machine learning algorithm that minimizes structural risk to deal with the classification problem of binary samples. Based on the limited sample information, it seeks a balance between the complexity of the model and the learning ability. Get the best promotion (generalization) ability. The nonlinear SVM adopts the kernel function mapping method to map the original sample space to the dimensional space, and finds a hyperplane to correctly classify the samples, so that the interval between the positive and negative samples is the largest.

For crop video images, the distribution of individual pixels and their values is continually evaluated.

Sometimes it will be in a general background state: sometimes it may be the shadow of a swinging plant; sometimes it can be part of the plant itself. Therefore, we can give the pixel (x, y) the value of $i_{x,y}$ is the weight of crop $c_{x,y}$, field $f_{x,y}$ and shadow $s_{x,y}$ and:

$$i_{x,y} = w_{x,y} \cdot (c_{x,y}, f_{x,y}, s_{x,y}) \tag{1}$$

These distributions are labelled subscripts and are emphasized as they differ from other pixels. For example, some parts of the image correspond to plants, and other parts are dark stripes between plants. $\Theta = \{\omega_l, \mu_l, \sum_l : l \in \{c, f, s\}\}$ is defined as a parameter of the pixel (x, y) model, such as $w_{x,y} = (\omega_c, \omega_f, \omega_s)$, $f_{x,y} \sim N(\mu_f, \sum_f)$, and the like. For the sake of clarity, we will ignore the subscript x, y of these parameters below. However, it should be clear that there are different sets of parameters for the pixels at position x, y. i is a pixel value and L is a random variable representing the pixel number in the image. Our model defines this probability as:

$$P(L = l, I(x, y, t) = i \mid \Theta) = \omega_l \cdot (2\pi)^{\frac{2}{d}} \left|\sum\right|^{-\frac{1}{2}} \exp\{-\frac{1}{2}(i - \mu_l)^T \sum_l^{-1} (i - \mu_l)\} \tag{2}$$

Among them, $I(x, y, t)$ is the instantaneous pixel value of the pixel (x, y) at time t. Assuming these probabilities, we can classify the pixel values, i.e. we choose class l with the highest posterior probability of $I(x, y, t)$.

RESULTS

Experimental design and analysis

Experimental environment

Table 1

Hardware Configuration Table

Model	To configure	Number	Remarks
Inter(R)Core(TM)i5-4000U	· CPU Main Frequency 1.6GHZ · 8GB Memory*1 · 500GB Hard Disk · 64-bit operating system	1	nothing

Application of probability learning pixel classification in shadow processing of agricultural plant video images

The concept of online learning is part of incremental learning. The basic idea is to learn the image features of the newly added samples, so that the model perceives the environmental changes in the device deployment area, solves the disadvantages of the algorithm model in the previous system, and improves the accuracy and robustness of the algorithm. Online learning is ideal for applications where the sample continues to grow and is used for iterative updates of the model. Most organizations now apply offline trained models and deploy them online for prediction or classification. The model trains and learns the new data on the line. After collecting the new data in the background, the new data is integrated with the previous data before training. Updating the model in this way not only wastes the storage space of the machine, but also wastes a lot of training time compared to the incremental training method. In the online learning phase of the system, the video server sends the detected image to the client for Alarm information, and the client user determines the result. If the server determines that there is no pedestrian image as a pedestrian, it is a false check. The client marks this image as a negative sample and sends it to the cloud server. When the cloud model is trained again, the information of the new sample set can be learnt, enhancing the model's effect on pedestrian detection in this context in continuous learning.

The offline training module is a model that is pre-trained and generated by the sample set before the model goes online. The model generated by the pre-training is not specific to the detection scenario. Before offline training of the algorithm, it is needed to build an initial version of the sample library, including video frames (positive samples) containing pedestrians or other targets and video frames (negative samples) that do not contain people or other targets. In order to obtain a good classifier, a certain number and quality of sample sets representing the environmental characteristics of the subordinate areas of the monitoring equipment are required. These sample sets include states in various situations as much as possible. For example, negative samples are used to capture images of different illuminations and angles in the same region, while positive samples should be collected from pedestrian images of different ages, genders, and regions.

In the collaborative training mechanism offline training module, this paper adopts the INRIA pedestrian detection data set with more comprehensive illumination conditions and human gestures in the picture, including 1218 negative sample images and 614 positive sample images. Each picture in this dataset is calibrated for the pedestrian area, and a rectangular frame is drawn, and the fixed point coordinates, the length and width of the rectangle on the rectangular frame are recorded. In order to get better results when using INRIA dataset, this paper pre-processes the original data, that is, 10 images of 64*128 size are randomly cut out from each original image, which increases the number of images. The number of original training sets also increases the diversity of the original training set.

The model training process is as shown in the following figure: Firstly, the training sample is cut to the appropriate size, and the image is selected by the histogram of oriented gradients (HOG). When the feature selection is performed, the detection sub-parameter file is generated according to the specific sample set, and the training is performed.

The model is saved locally. According to the HOG feature extraction process, each picture in the sample set is extracted into a one-dimensional vector, and all the images generated by the image are involved in the training of the SVM. Before the SVM is trained, the corresponding parameters are selected according to actual needs, and the parameters are set and then started. Perform SVM model training. To test the work of the shadow removal method, a continuous crop video stream is taken. This video stream is processed on the Windows operating platform of memory 1G and CPU 2.8GHZ using MATLAB 7.5. Processing data indicates that the pixels of the shadows and fields are relatively concentrated, while the pixels of the plants are relatively discrete. In order to distinguish the shadow from the plant, the pixel model and the incremental EM are determined.

In Figure 1, 47 frames, 194 frames, and 258 frames of the video, respectively, the shadow portion in each frame is determined by the probability learning pixel classification method, and then replaced with the corresponding field pixel value. From the examples, it can be seen that our real-time method has a good shadow removal capability, which paves the way for more sophisticated processing in various farmland applications.

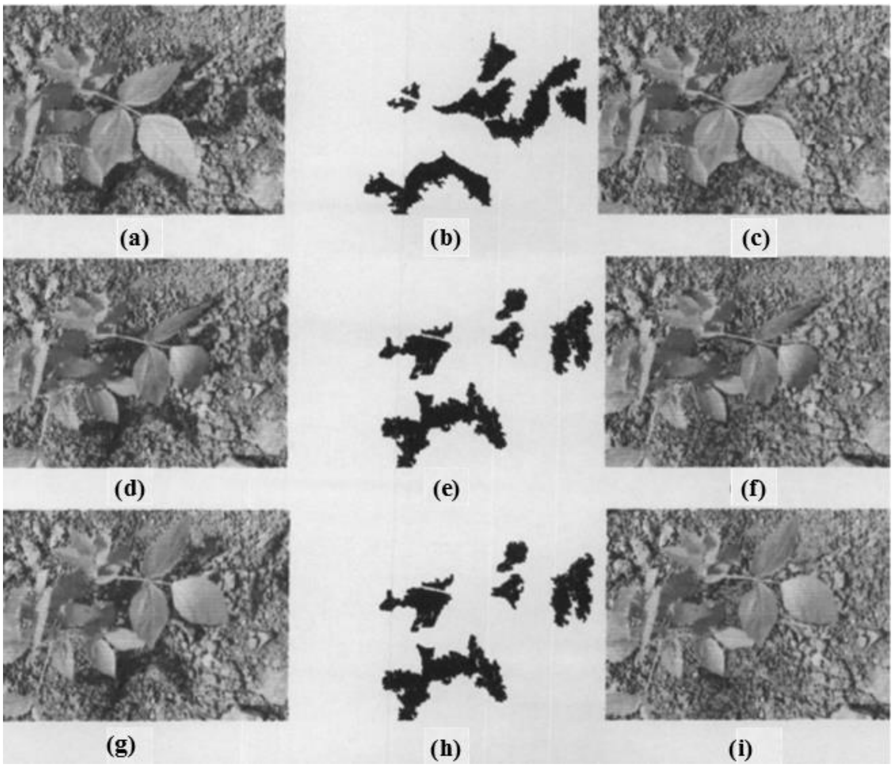

Fig. 1 - (a) Shadow detection (c) Shadow removal image (d) Shadow detection (f) Shadow removal image (g) Shadow removal image (h) detection of 258 frame (h) Shadow removal image (i)

Algorithm and model performance experiment and result analysis

Transaction response time: The time interval after the thread requests a video frame from the NVR to return to the video frame and write to the local disk.

The experimental results of Scheme 1 are analyzed as follows:

Table 2

Number of concurrent threads and corresponding time

	1	2	3	4
Transaction Maximum Response Time (ms)	874	1403	2334	2868
Transaction minimum response time (ms)	130	284	392	573
Transaction average response time (ms)	502	843.5	1363	1720.5

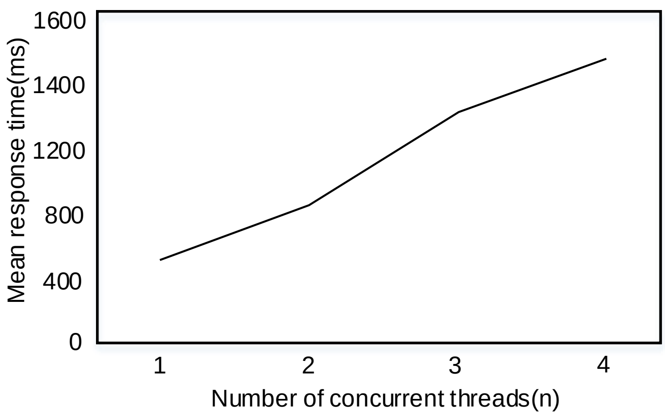

Fig. 2 - The relationship between the average response time and the number of concurrent threads

As can be seen from Figure 2, the average response time of a transaction has a tendency to increase as the number of concurrent threads increases. Analysis: Since the Haikang SDK (Software Development Kit) function interacts with the NYR to obtain images, when the number of concurrent threads increases, the degree of concurrency supported by the NVR is insufficient to cope with multiple threads requesting video frames at the same time, that is, the NVR delays when processing these requests.

There is the phenomenon that the operation of capturing a picture cannot be completed within a prescribed time interval of the program, and an error occurs. Limiting program capture performance is the degree of parallelism supported by the NVR. The experimental results of Scheme 2 are analyzed as follows:

Table 3

Number of concurrent threads and response time

	1	2	3	4
Transaction Maximum Response Time (ms)	532	590	658	730
Transaction minimum response time (ms)	50	68	79	106
Transaction average response time (ms)	291	329	368.5	418

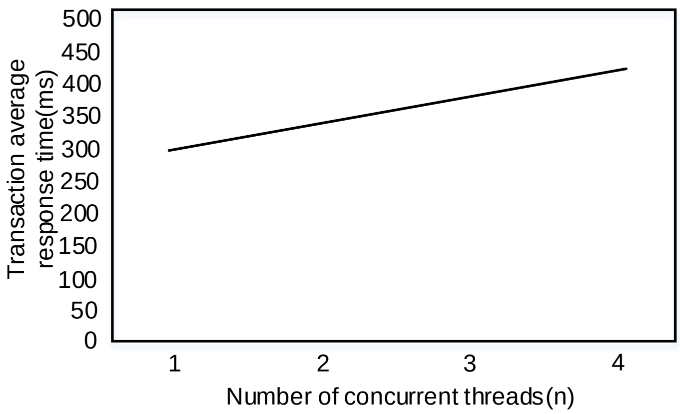

Fig. 3 - The relationship between the average response time and the number of concurrent threads

As shown in Figure 3, it can be seen that the transaction response time is increasing with the increase of the capture sub-thread. Analysis: In this scheme, the second callback is set in the callback function of the main thread, and the video stream obtained by the main thread from the NVR is decoded and stored locally, and the decoding process is also obtained from the NVR. The video stream is decoded into the YUV format. The process of initial decoding is also dependent on the NVR, and the NVR performs linear execution internally when it is converted to the YUV format. As the number of channel threads increases, the time interval for data snooping on each thread increases. Therefore, when the number of server-side channels is greatly expanded, the capture scheme based on the decoding callback will generate a long delay. This method cannot be applied to a specific system. The results of the third experiment are analyzed as follows:

Table 4

Number of concurrent threads and response time

	1	2	3	4
Transaction Maximum Response Time (ms)	28	29	29	30
Transaction minimum response time (ms)	13	14	19	15
Transaction average response time (ms)	20	23	24	23

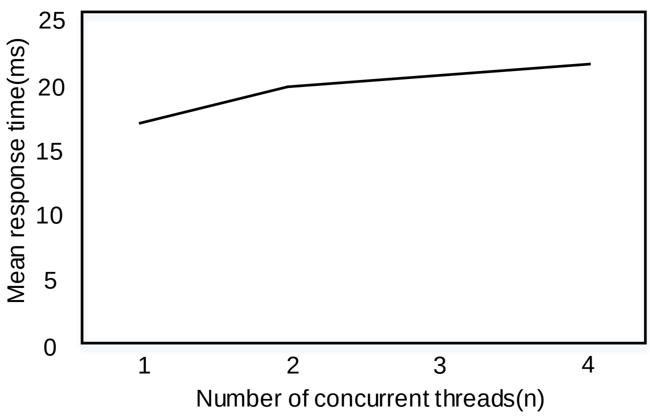

Fig.4 - The relationship between the average response time and the number of concurrent threads

The experiment shows that the average capture time does not fluctuate randomly with the increase of the number of channels, and the response time of the transaction is stable.

This experiment is simulated on VS2010IDE. By comparing the effects of traditional SVM training model and incremental SVM training model, the performance of incremental SVM training results for pedestrian detection is verified and suitable for use in the system. In this experiment, the model is based on offline training. The support vector set is set to SA_SV. Then, during the running of the system, the image of the pedestrian appears in the picture as the new sample B.

The experimental results of the distribution of samples and the number of iterations are as follows:

Table 5

Comparison Table of Detection Accuracy between Traditional Algorithms and Online Learning Algorithms

Classification number	**training set**	**New Sample Set**	**traditional algorithm**		**Online Learning Algorithms**	
			Time/s	accuracy rate	Time/s	accuracy rate
2	Initial sample set	1832	976.5	83%		
	New Sample Set 1	100	1024.6	83.3%	18.3	83.3%
	New Sample Set 2	200	1119.1	84.2%	32.3	85.2%
	New Sample Set 3	200	1203.5	85.4%	31.2	85.9%
	New Sample Set 4	200	1312.3	85.6%	33.2	86.5%
	New Sample Set 5	200	1429.6	86.1%	34.3	86.7%

The number of iterations of the algorithm can be adjusted according to the needs of the online training. According to the experimental observation, the number of iterations will affect the accuracy of the algorithm to some extent. The relationship is as shown below:

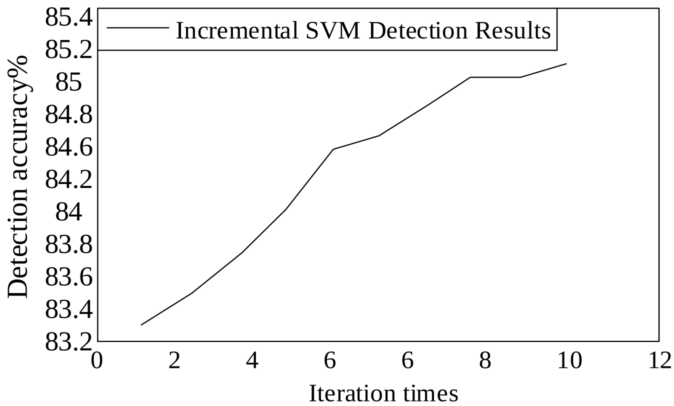

Fig. 5 - The relationship between the detection effect of incremental SVM and the number of iterations

The above results are analyzed as follows: Online learning can greatly shorten the training time, and can also effectively improve the accuracy of the training model detection. As the number of online training iterations increases, it can help to improve the detection accuracy of the generated model.

CONCLUSIONS

Scientific observation of crops is the basis of agricultural production and the application of computer technology in agricultural production can further improve the current situation of agricultural production. Therefore, this paper proposes a pixel classification based on the probability of real-time intelligent video learning, build the crops pixel model based on the cloud detection algorithm together, this algorithm to achieve HOG+SVM agriculture detection algorithm for the premise, the application of the idea of online learning system, that are related to the agricultural production, in turn, online update iteration model, enhance the model to improve the adaptability and agricultural environment detection accuracy.

A cloud collaborative detection mechanism is proposed to solve the problem of inaccurate offline model detection. The detected images are combined with the opinions of the client experts to form a new training sample and it is sent to the cloud model training server again.

The incremental training method is used to strengthen the detection model, which enhances the detection effect of the video server and dynamically improves the detection accuracy of the model in a specific scene.

This paper systematically studies intelligent video surveillance, and has achieved certain research results. However, there are still some shortcomings. In this paper, when online training of the model on the server, the online training requires continuous adjustment of the expert opinion of the test sample and then returns to the sample set on the remote server. Therefore, the experimental process of this part is carried out under the experimental environment of simulation.

REFERENCES

[1] Argandacarreras I, Kaynig V, Rueden C., (2017), Trainable Weka Segmentation: a machine learning tool for microscopy pixel classification. *Bioinformatics*, Vol.33, Issue 15, pp.2424;

[2] Arun P V, Buddhiraju K M, Porwal A., (2018), Integration of Contextual Knowledge in Unsupervised Subpixel Classification: Semivariogram and Pixel-Affinity Based Approaches. *IEEE Geoscience & Remote Sensing Letters*, Vol.29, Issue 99, pp.1-5;

[3] Girard F, Kavalec C, Cheriet F., (2019), Joint segmentation and classification of retinal arteries/veins from fundus images. *Artificial Intelligence in Medicine*, Vol.5, Issue 21, pp.4-7;

[4] Groot H G J, Oostdijk A, Van Persie M., (2017), Cloud and Shadow Detection using Sequential Characteristics on Multi-Spectral Satellite Images. *Electronic Imaging*, Vol.2017, Issue 13, pp.87-94.

[5] Hadiuzzaman M, Haque N, Rahman F., (2017), Pixel-based heterogeneous traffic measurement considering shadow and illumination variation. *Signal Image & Video Processing*, Vol.11, Issue 3, pp.1-8;

[6] Hou B, Kou H, Jiao L., (2017), Classification of Polarimetric SAR Images Using Multilayer Autoencoders and Superpixels. *IEEE Journal of Selected Topics in Applied Earth Observations & Remote Sensing*, Vol.9, Issue 7, pp.3072-3081;

[7] Li J, Khodadadzadeh M, Plaza A., (2017), A Discontinuity Preserving Relaxation Scheme for Spectral–Spatial Hyperspectral Image Classification. IEEE Journal of Selected Topics in Applied Earth *Observations & Remote Sensing*, Vol.9, Issue 2, pp.625-639.

[8] Majdar R S, Ghassemian H., (2017), A probabilistic SVM approach for hyperspectral image classification using spectral and texture features. *International Journal of Remote Sensing*, Vol.38, Issue 15, pp.4265-4284;

[9] Nan M, Zhu R, Li Y., (2018), Deshadowing of Urban Airborne Imagery Based on Object-Oriented Automatic Shadow Detection and Regional Matching Compensation. *IEEE Journal of Selected Topics in Applied Earth Observations & Remote Sensing*, Vol.11, Issue 99, pp.1-21;

[10] Rashno A, Nazari B, Sadri S., (2017), Effective pixel classification of Mars images based on ant colony optimization feature selection and extreme learning machine. *Neurocomputing*, Vol.226, Issue 89, pp.66-79;

[11] Sharma A, Liu X, Yang X., (2018), Land cover classification from multi-temporal, multi-spectral remotely sensed imagery using patch-based recurrent neural networks. *Neural Networks the Official Journal of the International Neural Network Society*, Vol.10, Issue 5, pp.346;

[12] Skakun S, Kussul N, Shelestov A Y., (2016), Efficiency Assessment of Multitemporal C-Band Radarsat-2 Intensity and Landsat-8 Surface Reflectance Satellite Imagery for Crop Classification in Ukraine. *IEEE Journal of Selected Topics in Applied Earth Observations and Remote Sensing*, Vol.9, Issue 8, pp.3712-3719;

[13] Tatar N, Saadatseresht M, Arefi H., (2018), A Robust Object-Based Shadow Detection Method for Cloud-Free High Resolution Satellite Images Over Urban Areas and Water Bodies. *Advances in Space Research*, Vol.7, Issue 8, pp.77-98;

[14] Tegolo D, Tegolo D., (2016), A multiscale approach to automatic and unsupervised retinal vessel segmentation using Self-Organizing Maps. *International Conference on Computer Systems & Technologies*. ACM, Vol.47, Issue 13, pp.26-52;

[15] Tolstik T, Marquardt C, Matth?Us C., (2014), Discrimination and classification of liver cancer cells and proliferation states by Raman spectroscopic imaging. *The Analyst*, Vol.139, Issue 22, pp.6036-6043;

[16] Wan S, Gong C, Zhong P., (2019), Multiscale Dynamic Graph Convolutional Network for Hyperspectral Image Classification. *IEEE Transactions on Geoscience and Remote Sensing*, Issue 99, pp.1-16;
[17] Wang P, Hu X, Li Y., (2016), *Automatic cell nuclei segmentation and classification of breast cancer histopathology images. signal processing*, Vol.122, Issue 9-10, pp.1-13;
[18] Wang W, Zhang J, Wu W., (2018), *An Automatic Approach for Retinal Vessel Segmentation by Multi-Scale Morphology and Seed Point Tracking. Journal of Medical Imaging and Health Informatics*, Vol.77, Issue 12, pp.26-52;
[19] Windrim L, Ramakrishnan R, Melkumyan A., (2018), A Physics-Based Deep Learning Approach to Shadow Invariant Representations of Hyperspectral Images. *IEEE Trans Image Process,* Vol.21, Issue 99, pp.665-677;
[20] Xiao-Bing H U, Rong-Fang Z, Xing Y E., (2017), Characteristic indexes of floc structure in activated sludge based on dimensionality reduction methods. *China Environmental Science*, Vol.37, Issue 5, pp.1759-1768;
[21] Xiao-Hong W, Yu-Qian Z, Miao L., (2015), Automatic Segmentation for Retinal Vessel Based on Multi-scale 2D Gabor Wavelet. *Acta Automatica Sinica*, Vol.41, Issue 5, pp.970-980;
[22] Xu M, Zhu J, Lv P., (2017), Learning-based Shadow Recognition and Removal from Monochromatic Natural Images. *IEEE Transactions on Image Processing*, Vol.26, Issue 12, pp.5811-5824.
[23] Yan X, Lu Y, Liu L., (2018), General Meaningful Shadow Construction in Secret Image Sharing. *IEEE Access*, Vol.6, Issue 99, pp.1-1;
[24] Yang J, Wang C, Cai G., (2016), Discrimination of liver cancer in cellular level based on backscatter micro-spectrum with PCA algorithm and BP neural network // SPIE/COS Photonics Asia. *International Society for Optics and Photonics*, Vol.22, Issue 31, pp.42-71;
[25] Yang S, Feng Z, Wang M., (2018), Self-Paced Learning-Based Probability Subspace Projection for Hyperspectral Image Classification. *IEEE Transactions on Neural Networks & Learning Systems*, Vol.24, Issue 99, pp.1-6.